[CANCER RESEARCH 64, 789–794, February 1, 2004]

Advances in Brief

Simultaneous Suppression of Epidermal Growth Factor Receptor and c-erbB-2 Reverses Aneuploidy and Malignant Phenotype of a Human Ovarian Carcinoma Cell Line

Svetlana D. Pack,[1] Özgül M. Alper,[5] Kurt Stromberg,[2] Meena Augustus,[3] Metin Özdemirli,[6] Anne M. Miermont,[7] Greg Klus,[7] Marek Rusin,[4] Rebecca Slack,[8] Neville F. Hacker,[9] Thomas Ried,[3] Zoltan Szallasi,[10] and Özge Alper[7]

[1]Laboratory of Immunopathology, National Institute of Allergy and Infectious Diseases, [2]Division of Therapeutic Proteins, Office of Therapeutic Research and Review, Center for Biologics Evaluation and Research, Food and Drug Administration, [3]Genetics Branch, Center for Cancer Research, and [4]Laboratory of Human Carcinogenesis, National Cancer Institute, NIH, Bethesda, Maryland; [5]Institute for Molecular and Human Genetics, [6]Laboratory of Pathology, [7]Department of Oncology, and [8]Department of Biostatistics, Vincent T. Lombardi Cancer Center, Georgetown University Medical School, Washington DC; [9]Gynaecological Cancer Center, Royal Hospital for Women, New South Wales, Sydney, Australia; and [10]Children's Hospital Informatics Program, Harvard Medical School, Boston, Massachusetts

Abstract

Coexpression of epidermal growth factor receptor (EGFR) and c-erbB-2 in 47–68% of ovarian cancer cells indicate their strong association with tumor formation. We examined the effects of simultaneous antisense- or immunosuppression of EGFR and c-erbB-2 expression on the invasive phenotype, aneuploidy, and genotype of cultured human ovarian carcinoma cells (NIH:OVCAR-8). We report here that suppression of both EGFR and c-erbB-2 results in regression of aneuploidy and genomic imbalances in NIH:OVCAR-8 cells, restores a more normal phenotype, and results in a more normal gene expression profile. Combined with cytogenetic analysis, our data demonstrate that the regression of aneuploidy is due to the selective apoptosis of double antisense transfected cells with highly abnormal karyotype.

Introduction

Simultaneous modulation of multiple targets is a promising direction in modern cancer therapy. We chose suppressing two epidermal growth factor receptors, epidermal growth factor receptor (EGFR) and c-erbB-2, for several reasons. First, they are both frequently overexpressed and/or amplified in human tumors, including ovary (1). Second, induction of these receptors is known to suppress apoptosis, whereas their inhibition induces programmed cell death (2). Third, both receptors have been targeted by either small molecule inhibitors (Iressa) or antibodies (Cetuximab, Herceptin) and have shown encouraging results in clinical trials (3). Finally, previous studies have shown that suppression of either receptors by AS methodology indicated a significant, although incomplete, reversion of the malignant phenotype in human ovarian cancer cells. In particular, NIH:OVCAR-8 cells stably transfected with an antisense (AS)-EGFR expression showed reduced proliferation and induction of differentiation (4). However, despite their reduced capacity for proliferation and tumor formation in nude mice (4), AS-EGFR cells formed colonies in soft agar with an incidence similar to parental cells (unpublished observation). On the other hand, transfection of NIH:OVCAR-8 cells with an inducible AS-c-erbB-2 expression vector resulted in inhibition of cell growth and colony formation in soft agar (5). In this article, we examined the effects of simultaneous antisense- and immunosuppression of EGFR and c-erbB-2 on the invasive phenotype, aneuploidy, and genotype, and we demonstrated that the simultaneous suppression of EGFR and c-erbB-2 not only resulted in a less malignant phenotype but also selectively triggered recapitulation of the cells with a more normal karyotype in a human ovarian cancer cell line.

Materials and Methods

Selection of Clones. NIH:OVCAR-8 cell line was a gift from Dr. Thomas C. Hamilton (Fox Chase Center, Philadelphia, PA). Cells were cultured in Improved Minimum Essential Medium (IMEM) containing 10% fetal bovine serum. The AS-expressing vector for AS-c-erbB-2 (pRC/CMV/AS 5′) and control vector (pRC/CMV) were kindly provided by Dr. Shoshana Segal (NIH/National Cancer Institute). The AS-expressing vector for EGFR (pCDNA3.1/AS-EGFR) was constructed as previously described using pCDNA3.1 zeo (Invitrogen Corporation, San Diego, CA; Ref. 4). Parental 8A1 cells were stably transfected with vectors expressing AS-EGFR and/or AS-c-erbB-2 (pCDNA3.1/AS-EGFR and/or pRC/CMV/AS-c-erbB-2, respectively) and control vectors, Ev-Cv (pCDNA3.1 and/or pRC/CMV, respectively). To verify the identity of the plasmids used in transfections, we sequenced AS-EGFR and AS-c-erbB-2 inserts using primers complementary to the vector sequences and ABI PRISM BigDye Terminator Cycle Sequencing kit (PE-Applied Biosystems; Foster City, CA) according to the manufacturer's protocol. Sequencing products were separated on ABI Prism 377 DNA Sequencer (PE-Applied Biosystems).

Treatment of Cells with Cetuximab, Herceptin, and Prostaglandin E_2 (PGE_2). Parental 8A1 cells were treated individually and simultaneously with clinical grade monoclonal antibodies Cetuximab (C225; Imclone Systems Incorporated, New York, NY) and Herceptin (trastuzumab; Genentech, Inc., South San Francisco, CA) at concentrations of 0.1–0.5 and 0.5–4.4 mg/ml, respectively, in IMEM medium with 5% fetal bovine serum for 24–72 h either in plastic culture dishes or on glass coverslips. After simultaneous treatment of parental 8A1 cells with Cetuximab (0.4 mg/ml) and Herceptin (3.0 mg/ml) for 48 h, cells were washed with serum-free medium and treated with PGE_2 (10–20 μM; Sigma) for 24–48 h in serum-free medium. Control cells were treated with ethanol.

Detection of Apoptosis and Ploidy. Apoptosis was detected by Annexin V-FITC and propidium iodide staining using AnnexinV-FITC Apoptosis kit (PharMingen, San Diego, CA). Twenty thousand cells were analyzed on FACSort (Becton Dickinson, San Diego CA). Results were analyzed using FCS Express (De Novo Software, Thornhill, Ontario, Canada). Cells were stained with propidium iodide and analyzed in duplicate with and without human WBC as an internal standard. One hundred thousand cells were analyzed on FACSort. DNA index and ploidy were determined using ModFitLT software (Verity Software, Topsham, ME).

Received 7/3/03; revised 12/3/03; accepted 12/11/03.

Grant support: Charles and Ella O. Latham Trust, the Alexander C. and Tillie S. Speyer Foundation, and the Gynecological Cancer Fund of the Royal Hospital for Women Foundation, Sydney, Australia. M. Rusin is a recipient of Union Internationale Contre le Cancer Fellowship Award, 9/2000. The Microscopy and Imaging, Biostatistics, and Flow Cytometry Shared Resources of Lombardi Cancer Center is partially supported by NIH Grants 2P30-CA-51008 (Cancer Center Support Grant, to Lombardi Cancer Center) and 1S10 RR15768-01.

The costs of publication of this article were defrayed in part by the payment of page charges. This article must therefore be hereby marked *advertisement* in accordance with 18 U.S.C. Section 1734 solely to indicate this fact.

Notes: Supplementary data for this article can be found at Cancer Research Online (http://cancerres.aacrjournals.org). M. Augustus is currently at Avalon Pharmaceuticals, Germantown, Maryland. M. Rusin is currently at the Department of Tumour Biology, Center of Oncology, Maria Sklodowska-Curie Memorial Institute, Gliwice, Poland.

Requests for reprints: Özge Alper, National Institute of Health, Building 10, Room 5D37, 9000 Rockville Pike, Bethesda, Maryland 20892-1414. E-mail: oa4@georgetown.edu.

Protein Analysis. Cells (1×10^6) in tissue culture were lysed in radioimmunoprecipitation assay buffer [250 mM NaCl, 20 mM Na_2HPO_4, 1% Triton, 1% deoxycholic acid, 0.1% SDS, protease inhibitor (Complete Mini; Roche), 1 mM $NaVO_4$]. Total protein (800 μg/ml) was immunoprecipitated with the following mouse monoclonal antibody specific to phosphotyrosine (4G10; Upstate, Lake Placid, NY), resolved by 4–12% SDS-PAGE gels and transferred to nitrocellulose sheets. Blotting was performed with anti-EGFR and anti-c-erbB-2 antibodies (Ab-12 and Ab-17; NeoMarkers, Fremont, CA). The expression of poly(ADP-ribose) polymerase (PARP), bcl-2, and actin was analyzed by Western blot using 20–40 μg protein/lane. Blotting was performed using anti-PARP mouse monoclonal antibody (MoAb, Ab2; Oncogene Research, Boston, MA) according to manufacturer's instructions, anti-bcl-2 PoAb (N-19; Santa Cruz Biotechnology, Santa Cruz, CA) and anti-actin MoAb (I19; Santa Cruz Biotechnology). Bands were visualized with secondary horseradish peroxidase-conjugated antibodies and the enhanced chemiluminescence system (Amersham Pharmacia). Matrix metalloproteinase-9 activity was measured by zymography analysis. Briefly, cells were grown to 80% confluence in complete medium and then incubated for 72 h in serum-free medium. Aliquots of serum-free media were analyzed by gel electrophoresis. Dried gels were scanned by use of ChemiImager 5500 (α Innotech Corporation, San Leandro, CA).

Matrigel Outgrowth, Immunohistochemical, and Indirect Immunofluorescent Staining. Cells were seeded on glass coverslips in 12-well plates coated with 0.5 ml of Matrigel (10 mg/ml; kindly provided by Dr. Hynda Kleinman, National Institute of Dental and Craniofacial Research, Bethesda, MD). The plates were incubated at 37°C in IMEM medium (Life Technologies, Inc.) containing 10% fetal bovine serum for various time periods. After the nonadherent cells were removed by washing gently with PBS, adherent cells were fixed with 70% methanol for 5 min at room temperature and stained with Giemsa (Sigma, St. Louis, MO). Fibronectin (FN) expression was detected by staining the cells with anti-FN MoAb (Transduction Laboratories, Lexington, KY) and FITC-labeled secondary MoAb. The images were analyzed using an Olympus IX-70 laser confocal scanning microscope equipped with an Olympus 60x/1.4 N.A. objective lens. Paraffin sections for control and transfected cells were stained with antiprogesterone receptor MoAb (A6; Coulter Corporation, Miami, FL) using Dako Envision kit (Dako Corporation, Carpinteria, CA). The images were analyzed using an Olympus Vanox Microscope equipped with a Zeiss 25x/0.8 N.A. objective lens.

Comparative Genomic Hybridization (CGH) and Spectral Karyotype Analysis. CGH and spectral karyotyping were done as described previously (6). After one passage in culture after stable transfection or treatment of parental 8A1 cells with Cetuximab and Herceptin for 24 and 48 h, tumor cell lines were processed and analyzed by CGH, spectral karyotype, and specific chromosome paints (fluorescence *in situ* hybridization). Cells were arrested at mitosis by treatment with Colcemid (Life Technologies, Inc.) at 0.1 μg/ml for 1 h. Mitotic chromosome spreads were prepared, and spectral karyotype analysis was performed. For fluorescence *in situ* hybridization analysis, metaphases were hybridized using directly labeled locus specific probes for chromosomes 16 and 20 (Vysis, Downers Grove, IL).

Analysis of Differential Gene Expression. Cells were grown in duplicate in 150-mm dishes (Corning, Corning, NY), and RNA was isolated using TRIzol LS (Invitrogen, Carlsbad, CA) and then additionally purified using an RNeasy spin column (Qiagen, Valencia, CA). RNA eluted from the columns was immediately concentrated to ~3 $\mu g/\mu l$ using a Microcon 30 centrifugal filter device (Millipore, Bedford, MA) and stored at −80°C until used for microarray analysis.

cDNA microarrays containing ~6400 clones were obtained through a collaboration with the Cancer Genetics Branch at The National Human Genome Research Institute, NIH. CyDye-labeled cDNA was prepared from RNA and hybridized to microarrays as described online.[11] Arrays were scanned using an Agilent microarray scanner (Agilent Technologies, Palo Alto, CA), and expression ratios were determined using the Arraysuite software package,[12] which is a collection of software tools customized for analyzing cDNA microarrays, written as extensions to the IPLab image analysis software package (Scanalytics, Fairfax, VA) for the Apple Macintosh computer.

[11] Internet address: http://research.nhgri.nih.gov/microarray/index.html.
[12] Internet address: http://research.nhgri.nih.gov/microarray/image-analysis.html.

Results and Discussion

We cloned NIH:OVCAR-8 cells and for additional experimentation, we selected a subclone (labeled 8A1), with a high level of chromosomal aberrations, as indicated by CGH analysis (unpublished observation). After stable transfection of these parental 8A1 cells with AS-EGFR and/or AS-c-erbB-2 and the control Ev-Cv vectors, we selected several clones and verified the reduction of protein expression for EGFR and c-erbB-2 receptors by Western blot analysis of cell lysates (Fig. 1*A*). The 8A1, parental cells, as well as Ev-Cv, double vector control transfectants, expressed high amounts of EGFR and c-erbB-2, whereas E2 cells (AS-EGFR) expressed decreased EGFR and C7 cells (AS-c-erbB-2) expressed decreased c-erbB-2 (Fig. 1*A*). Double transfectants for AS-EGFR and AS-c-erbB-2, including clones E-C32.d and E-C32.2, expressed decreased levels of both EGFR and c-erbB-2 in comparison to parental 8A1 cells (Fig. 1*A*). These observations suggested that simultaneous suppression of EGFR and c-erbB-2 by antisense-expressing constructs was highly effective.

When grown on Matrigel, a naturally occurring basement membrane-like extracellular matrix, parental 8A1 cells and Ev-Cv control transfectants were polygonal in shape with interconnected cell clusters (Fig. 1*B*). In contrast, E-C32.d and E-C32.2 double-transfected clones were observed viable, spherical, single cells similar to normal ovarian cells (Fig. 1*B*). Zymography analysis showed a >3-fold decrease in secreted matrix metalloproteinase-9 by the double transfectants relative to the parental 8A1 cells (Fig. 1*C*). Thus, simultaneous

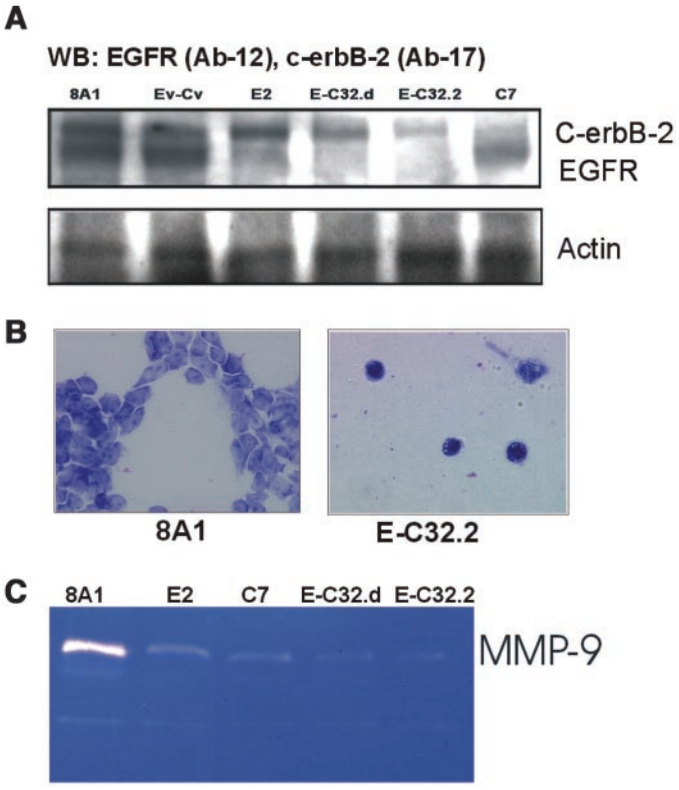

Fig. 1. Biological consequences of simultaneous suppression of epidermal growth factor receptor (EGFR) and c-erbB-2 in ovarian cancer cells. *A*, EGFR and c-erbB-2 protein expression in selected parental 8A1, control vectors for EGFR and c-erbB-2 (Ev-Cv), single antisense (AS)-EGFR (E2), AS-c-erbB-2 (C7), and double AS-EGFR/AS-cerbB-2 (E-C32.d, E-C32.2)-transfected antisense clones. Protein lysates were extracted and subjected to Western blot analysis. The data represent replicate analysis. *B*, Matrigel outgrowth of parental 8A1 and E-C32.2 double-transfectant cells. The images are the representative results of three independent experiments. *C*, matrix metalloproteinase-9 (MMP-9) activity in parental 8A1 cells compared with single and double transfectants by zymogram analysis when seeding an equal number of cells. The experiment was repeated three times.

suppression of EGFR and c-erbB-2 resulted in inhibition of invasive phenotype by a decrease in growth in Matrigel and matrix metalloproteinase-9 activity.

This significant reversal in phenotype prompted us to examine whether we can detect any consistent corresponding changes in the chromosomal profiles of the single and double AS-transfected clones relative to the parental 8A1 cells by molecular cytogenetic techniques, including fluorescence *in situ* hybridization and CGH. A direct chromosomal enumeration (after Giemsa staining) coupled with CGH data revealed a striking tendency for reduction of chromosomal aneuploidy in the double transfectants. The parental 8A1 cells had a ploidy range from 42 to 113 with the major clone having 58 chromosomes indicative of a significant chromosomal instability (Fig. 2, *A* and *B*). However, we observed a reduction in the chromosomal number, with clonal ploidy of 46–52 and 46–50 in the E-C32.d and E-C32.2 double-transfected clones, respectively (Fig. 2*F*; Supplementary Table 1). Consistent with the decrease in chromosome number, we observed a decrease in ploidy of E-C32.d and E-C32.2 double transfectants by fluorescence-activated cell sorting analysis as well (Supplementary Table 1). We expanded our analysis to CGH to view a global picture of all apparent chromosomal changes between the parental cells and the dual-transfected stable AS clones. To highlight these differences, we used DNA from parental 8A1 cells as a reference instead of DNA from normal donors (6). Parental 8A1 cells revealed a high level of genomic imbalances relative to normal cells as summarized in Supplementary Table 1. Our main interest was to see whether chromosomal imbalances often observed in ovarian cancer could be reversed by the simultaneous suppression of EGFR and c-erbB-2. Remarkably, we have found several examples. A consistent loss of chromosomes 5 and chromosomal region 11q23.3-qter was seen in the E-C32.d and E-C32.2 double transfectants in comparison to parental 8A1 cells, which had a gain of chromosome 5 (Supplementary Table 1). Gain of chromosome 5 is one of the earliest genetic events for human ovarian surface epithelial cells immortalized by HPV16-*E6E7* viral oncogenes (7). We also observed loss of chromosome 8q22-qter in E-C32.2 double transfected cells that was a gain in parental 8A1 cells (Supplementary Table 1). The amplification of c-myc on chromosomal region 8q24 (~30%) is a common finding in ovarian and other cancers (8). CGH data analysis showed a loss of chromosome 8q22-qter in E-C32.2 double transfectant (Supplementary Table 1). A loss of chromosome 20q was also observed (Supplementary Table 1, Fig. 2*G*). Interestingly, 40% of ovarian primary carcinomas also have a gain in copy number of chromosome region 20q (9). This region includes matrix metalloproteinase-9 (20q12.2-13.1), a putative oncogene, EEF1A2 (20q13), and a recently identified testis-cancer gene *BORIS* (10). *BORIS* is the first gene from the testis-cancer family that has oncogenic properties and maps to 20q13.2, a hot spot of amplification in many cancers, including ovarian cancer (11). A gain of chromosome region 18q23.1-qter in the E-C32.2 double transfectants was also seen. In contrast, this region is frequently lost (~33%) in ovarian carcinomas and was also lost in parental 8A1 cells and Ev-Cv control transfectants (12).

Using cDNA microarray technology, we also investigated whether the reversal of cancer-associated chromosomal changes is associated with the reversal of cancer associated gene expression changes as well. We observed a consistent and marked up-regulation of insulin growth factor binding protein-3 expression (7p13-p12) in E-C32.d and E-C32.2 double transfectants (Supplementary Table 2). Interestingly, this finding correlated with the loss of 7p13 in parental 8A1 cells by CGH analysis (Supplementary Table 1). Normal ovarian epithelial cells have been shown to express high levels of Insulin growth factor binding protein-3 that is also associated with apoptosis in p53-negative cells (10). Our findings in this model are consistent with an insulin growth factor binding protein-3-induced apoptosis that eliminates highly aneuploid cells. We have also observed that the expression level of caspase-8-associated protein 2, a mouse apoptotic protein that is highly similar to FLICE-associated huge, and DNA-activated kinase mRNA were increased in E-C32.d and E-C32.2 double transfectants (Supplementary Table 2).

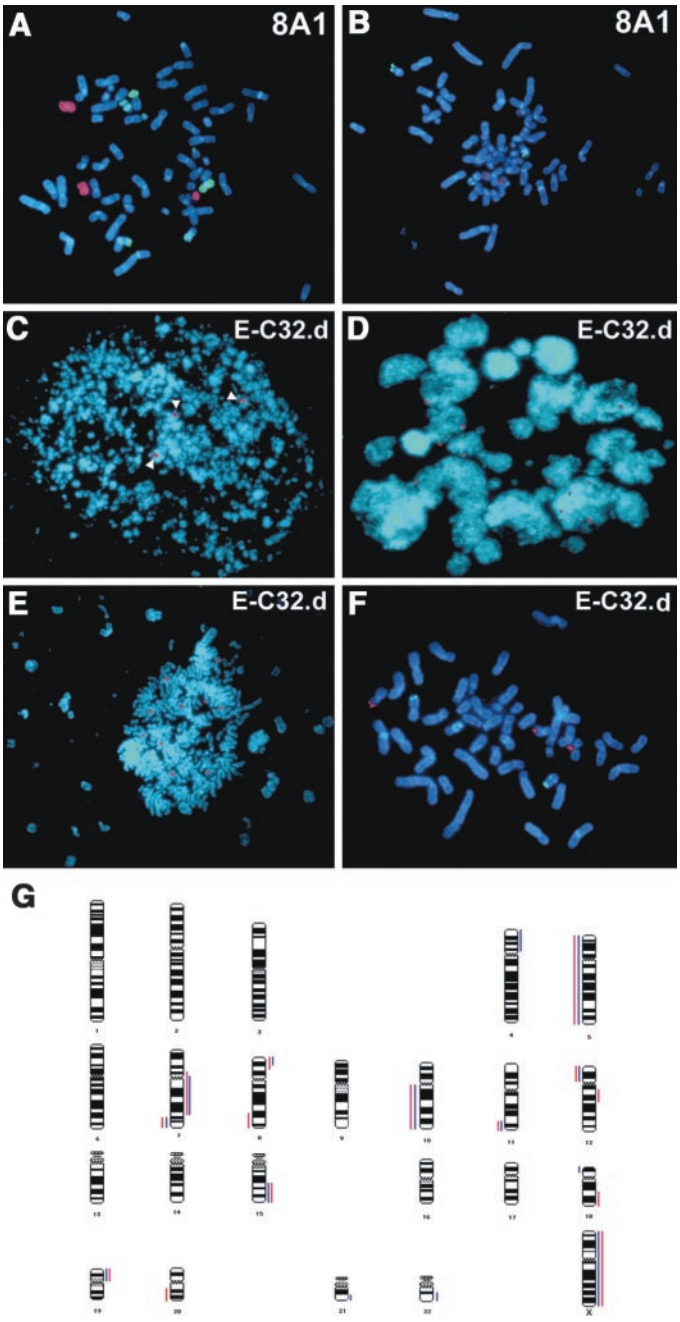

Fig. 2. Cytogenetic analysis of parental 8A1 cells and double-transfectant antisense clone E-C32.d and E-C32.2. Metaphase spreads of (*A*) 8A1 cells (58 chromosomes) after fluorescence *in situ* hybridization with chromosome 16 (*green*) and 20 (*red*) specific painting probes and (*B*; 61 chromosomes) with chromosome 16q (*green*) and 20q (*red*) locus-specific probes; *C–E*, multiple figures of apoptosis seen in the clone E-C32.d showing (*C*) chromosomal pulverization (note the presence of three copies of 20q probe). *Arrows* indicate 20q fluorescence *in situ* hybridization signals. *D*, nuclear fragmentation after endoreduplication (multiple copies of 20q probe can be seen); *E*, endoreduplication (octaploid cell with 12 copies of chromosome 20q probe); *F*, near-diploid metaphase spread (47 chromosomes) of E-C32.d cells with three copies of 20q locus-specific probe (*scale bar:* 100 μm). Results similar to figures (*C*, *D*, and *E*) double-transfectant E-C32.d clone were obtained also with E-C32.2 clone. *G*, summary of CGH analysis of E-C32.d and E-C32.2 double-transfected antisense clones compared with parental 8A1 cells. *Blue* and *red lines* represent E-C32.d and E-C32.2 double transfectants, respectively. *Lines to the left* of the chromosomes designate losses, whereas *lines to the right* display gains.

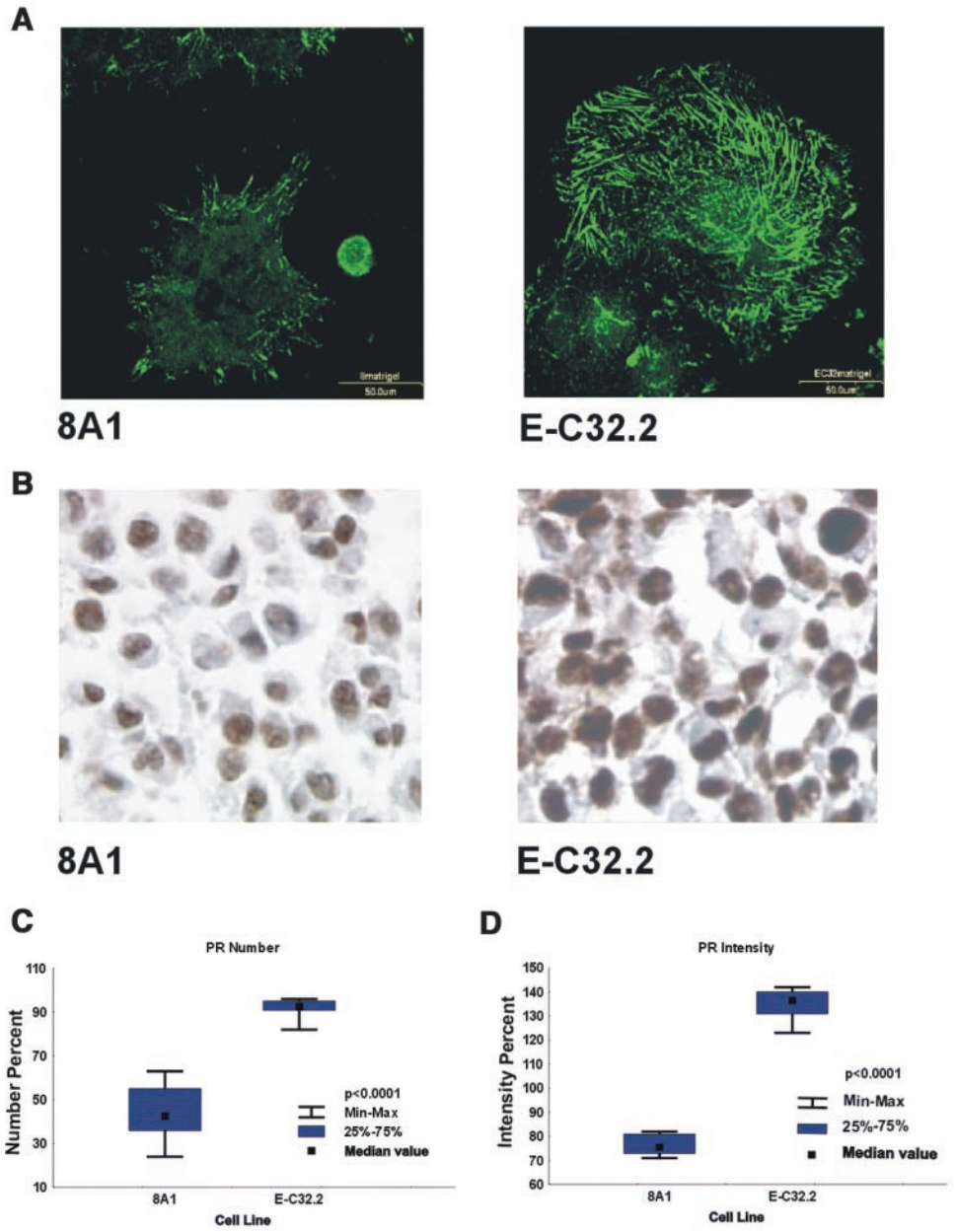

Fig. 3. Fibronectin and progesterone receptor (PR) expression. Immunofluorescent images of fibronectin distribution of parental 8A1 and double antisense-transfectant E-C32.2 cell clusters (*A*) when cultured on Matrigel. *Scale bar:* 50 μM. PR expression by immunohistochemical analysis in paraffin-embedded cell pellets of parental 8A1 cells and E-C32.2 double antisense-transfectant clone (*B*). For *A* and *B*, similar results to double antisense-transfectant E-C32.2 clone were obtained also with double-transfectant E-C32.d clone. A nested ANOVA was performed to determine whether the transfectants differ in terms of the number of cells stained (*C*) or the intensity of the PR staining (*D*). The E-C32.2 double transfectant is determined to be significantly different from the parental 8A1 cells if the P is <0.05. The results are plotted using *box plots* with limits for the medians, quartiles, and ranges of the observations.

Interestingly, caspase-8, which maps to 6q16.1, is an initiator of the death receptor pathway that activates apoptotic substrates, including PARP and DNA-activated kinase (13). Differential gene expression analysis also showed up-regulation of FN mRNA in E-C32.d and E-C32.2 double transfectants in contrast to parental 8A1 cells (Supplementary Table 2). In addition, confocal laser scanning microscopic images indicated a significant difference in FN expression and distribution by immunofluorescence staining analysis. Parental 8A1 cells deposited relatively less FN localized mainly to the cell periphery (Fig. 3*A*). In contrast, E-C32.2 double transfectants had an increase in FN expression and fibrillogenesis occurred over the entire ventral cell surface. Our data correlates with studies showing the presence of FN throughout the stroma of normal ovarian tissue and the loss of FN in advanced ovarian tumors (14).

A decrease in progesterone receptor (PR) levels in ovarian adenocarcinomas and an increase in EGFR expression in comparison to benign, borderline, and normal ovarian tissues have been shown earlier (15). Therefore, we investigated PR expression in parental and double-transfected clones by immunohistochemical analysis. Double transfectants showed a significant increase in PR number ($P < 0.0001$; Fig. 3*C*) and intensity of staining ($P < 0.0001$; Fig. 3*D*) in E-C32.2 double transfectants compared with parental 8A1 cells (Fig. 3*B*). The significant increase in PR expression and induction of apoptosis by simultaneous inhibition of EGFR and c-erbB-2 are consistent with the results of the study showing a direct interaction of PARP with the DNA binding domain of human PR (16). This provides an insight into the cellular mechanisms of regulation of receptor tyrosine-kinase signaling pathway. PR-positive tumors are associated with an improved patient survival (17).

Our initial observation of the reversal of aneuploidy in ovarian cancer was so unexpected that we were eager to test whether we could reproduce the same phenomenon by the immunological inhibition of the same receptors. Remarkably, our findings in reduction of aneuploidy could be also induced by simultaneous treatment of parental 8A1 cells with Cetuximab and Herceptin. Our results showed a reduction in chromosome number with a modal number of 51 chromosomes in surviving cells 4 days after treatment (Supplementary

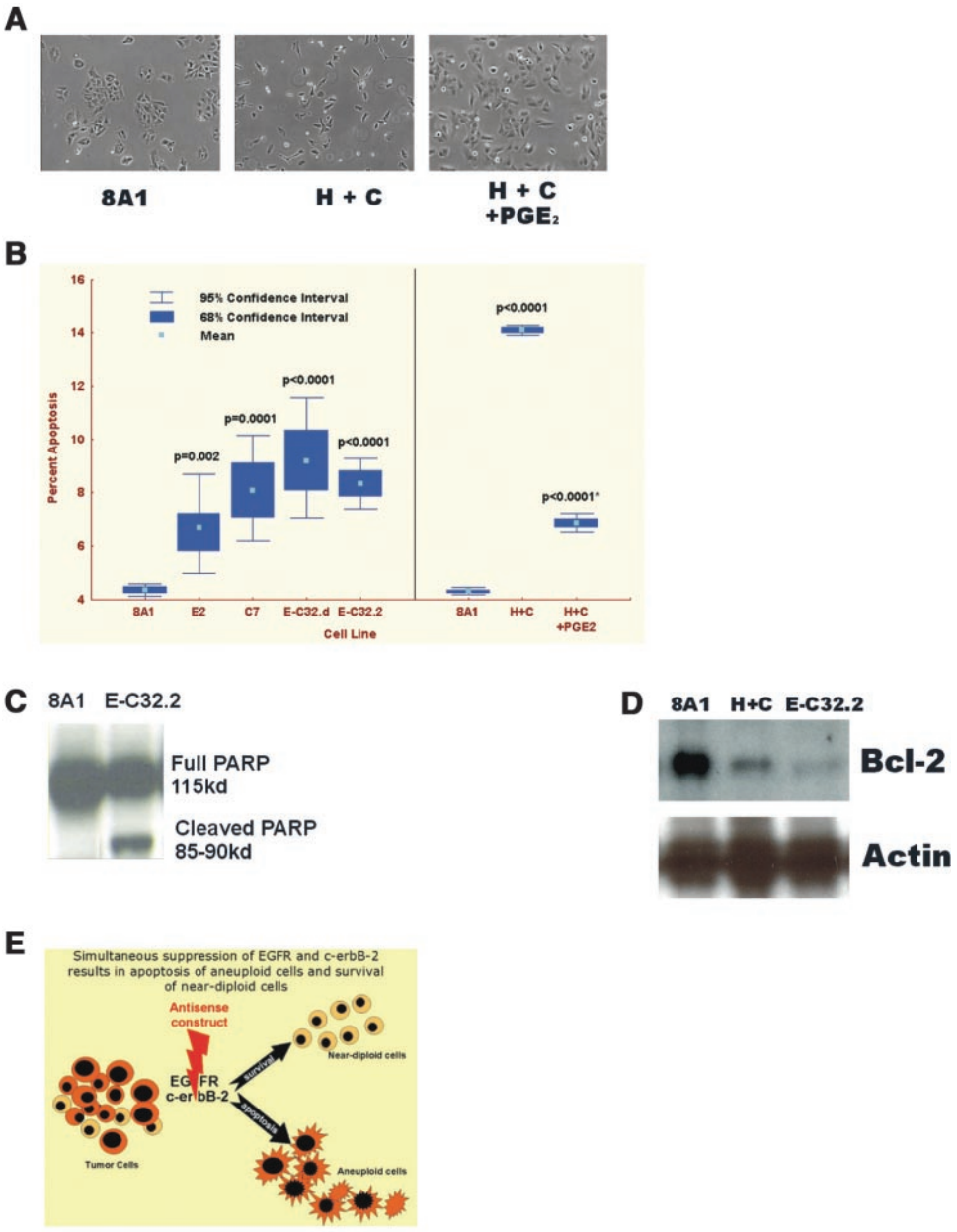

Fig. 4. Simultaneous suppression of epidermal growth factor receptor (EGFR) and c-erbB-2 altered cell morphology. *A*, cells showed a differentiated phenotype by simultaneous treatment of parental 8A1 cells with Cetuximab (C) and Herceptin (H) and the treated cells displayed similar morphology to parental 8A1 cells by the addition of prostaglandin E_2 (PGE_2). Images were taken with ×10 objective. This assay was repeated five times. *B*, apoptosis is determined by AnnexinV/propidium iodide staining and poly(ADP-ribose) polymerase (PARP) cleavage. Annexin V/propidium iodide staining was determined in parental 8A1, single (E2 and C7) and double antisense-transfectant (E-C32.d and E-C32.2) clones by fluorescence-activated cell sorting analysis. This analysis allowed flow cytometric quantitation of apoptosis occurring in parental cells (8A1; $n = 2$ in all groups), vector control (data not shown) cells, cells transfected individually with antisense (AS)-EGFR (E2) and AS-c-erbB-2 (C7) or simultaneously with AS-EGFR and AS-c-erbB-2 (E-C32.d and E-C32.2). Apoptosis was also determined in parental 8A1 cells treated simultaneously with Cetuximab (C) and Herceptin (H) and in additional PGE_2-treated cells. An ANOVA was implemented to determine whether a difference existed among any of the cell lines with pair wise comparisons using contrasts. *C*, PARP cleavage analysis showed two bands that were specific for full PARP (115 kd) and cleaved PARP (85–90 kd) in E-C32.2 double antisense-transfectant clone compared with parental 8A1 cells. A similar result was also obtained in E-C32.d double transfectant. Each result is representative of a total of three experiments. *D*, reduction in Bcl-2 expression by simultaneous blockade of EGFR and c-erbB-2. Western analysis showed reduction in bcl-2 expression in parental 8A1 cells simultaneously treated with Cetuximab (C) and Herceptin (H) and in E-C32.2 double transfectant compared with parental 8A1 cells. We obtained similar result in E-C32.d clone. The experiment was repeated twice. *E*, the hypothetical proposed model of the "bottleneck" genomic rescue through apoptosis and regression of aneuploidy in ovarian cancer cells after simultaneous suppression of EGFR and c-erbB-2.

Table 1). Reversal to the more normal karyotype was accompanied by a change in morphology after Cetuximab and Herceptin treatment. The dual-treated cells exhibited retracted morphology and did not form clusters compared with parental cells (Fig. 4*A*).

Such a reversal of the malignant karyotype is most readily explained by the selective death of those cells with a high level of aneuploidy. Therefore, as an obvious next step, we have investigated apoptotic events in our experimental system using AnnexinV/FITC cell surface (early apoptosis) and propidium iodide nuclear (late apoptosis) staining. A significant increase in apoptosis, when measured with by Annexin/propidium iodide staining, was observed in both single and double AS-transfected clones (Fig. 4*B*). Chromosomal analysis also revealed that a high percentage of cells (40%) in the E-C32.d clone, as indicated by chromosomal pulverization, was undergoing apoptosis (Fig. 2*C*) and nuclear fragmentation (Fig. 2*D*). Chromosomal endoreduplication and nondisjunction (Fig. 2*E*) were indicated by giant metaphase plates that were either blocked in mitosis or at the mitotic exit. In contrast, only 5% of the parental 8A1 cells were apoptotic (Fig. 4*B*). In addition, we have detected cleaved PARP expression in E-C32.d and E-C32.2 double transfectants (Fig. 4*C*) by Western analysis. PARP cleavage by caspase(s) occurs early in apoptosis, earlier on or soon after the appearance of internucleosomal fragmentation of DNA. Interestingly, we detected up-regulation of tankyrase in E-C32.d and E-C32.2 double transfectants by differential gene expression analysis (Supplementary Table 2). Tankyrase is a family member of the poly(ADP-ribosyl)ating proteins that has PARP activity (18). Although the underlying molecular events of these interactions remain unclear, it is speculated that PARP takes part mainly in interrelated events in the nucleus, including DNA repair, cell cycle regulation, and apoptosis, contributing to the maintenance of stability of the genome (13, 19). Taken together, we concluded that a subpopulation of E-C32.d and E-C32.2 double transfectants underwent apoptosis, whereas the majority of cells that was rescued from apoptosis had a near diploid chromosome content (46–50 in the case the E-C32.2 clone).

Again, we have tested whether we could reproduce the AS effect

with immunological inhibition of EGFR and c-erbB-2. We could induce a significant increase of apoptosis in the parental 8A1 cells by the simultaneous treatment of Cetuximab and Herceptin (Fig. 4*B*). To test the role of well-known apoptotic pathways, we have measured the level of an antiapoptotic protein bcl-2 under various conditions. The parental 8A1 cell line showed a high level expression that was down-regulated in the double transfected clone E-C32.2 and when the parental 8A1 cells were treated with a combination of Cetuximab and Herceptin (Fig. 4*D*). We were seeking to establish a stronger causative link between apoptosis and the observed effect of simultaneous suppression of EGFR and c-erbB-2. For this, we used PGE_2, an inhibitor of apoptotic pathways (20). As shown on Fig. 4*B*, PGE_2 significantly ($P < 0.0001$) inhibited the induction of apoptosis of dual Cetuximab and Herceptin treatment. This inhibition was accompanied by an increase in bcl-2 expression (data not shown). Furthermore, in addition to inhibiting apoptosis, PGE_2 also induced a reversal of morphology of dual Cetuximab/Herceptin-treated cells similar to the parental 8A1 cells (Fig. 4*A*). Thus, "genomic recovery," changes in morphology and induction of apoptosis, showed a strong correlation. This suggests that simultaneous inhibition of EGFR and c-erbB-2 induces apoptosis in cells that are aneuploid, whereas cells that are near-diploid or diploid survive and have a more normal karyotype (Fig. 4*E*).

This study is the first to show a regression from aneuploidy to a near-diploid state after dual suppression of EGFR and c-erbB-2 receptor expression in a human ovarian carcinoma cell line (Fig. 4*E*). In search of a possible mechanism, we detected a significant increase in apoptosis in the double transfectants as well as dual Cetuximab- and Herceptin-treated cells. Considering the intimate involvement of EGFR and c-erbB-2 in the regulation of apoptosis, a likely explanation of the reversal to a more normal karyotype is the reinduction of appropriate checkpoints. We are currently investigating the connections between EGFR and c-erbB-2 with the checkpoints and related regulatory pathways. We plan to examine the effects of a dual small interfering RNA (siRNA)-induced inhibition of these receptors in other cell lines and to explore the potential therapeutic relevance *in vivo*.

Acknowledgments

We thank Dr. Shoshana Segal (NIH/National Cancer Institute) for providing us with the antisense expression vector against c-erbB-2. We thank Victoria North and Jawad Issa (Tissue Culture Shared Resource, Lombardi Cancer Center, Washington DC) and acknowledge the assistance of Dr. Susette C. Mueller during the course of this work. We also thank the Microscopy and Imaging, Biostatistics, and Flow Cytometry Shared Resources of Lombardi Cancer Center. We also thank Imclone Systems Incorporation (New York) for providing us with Cetuximab.

References

1. Harlozinska, A., Bar, J. K., Sobanska, E., and Goluda, M. Epidermal growth factor receptor and c-erbB-2 oncoproteins in tissue and tumor effusion cells of histopathologically different ovarian neoplasms. Tumour Biol., *19:* 364–373, 1998.
2. Moulder, S. L., Yakes, F. M., Muthuswamy, S. K., Bianco, R., Simpson, J. F., and Arteaga, C. L. Epidermal growth factor receptor (HER1) tyrosine kinase inhibitor ZD1839 (Iressa) inhibits HER2/neu (erbB2)-overexpressing breast cancer cells in vitro and in vivo. Cancer Res., *61*:8887–8895, 2001.
3. Normanno, N., Campiglio, M., De, L. A., Somenzi, G., Maiello, M., Ciardiello, F., Gianni, L., Salomon, D. S., and Menard, S. Cooperative inhibitory effect of ZD1839 (Iressa) in combination with trastuzumab (Herceptin) on human breast cancer cell growth. Ann. Oncol., *13:* 65–72, 2002.
4. Alper, O., De, Santis, M. L., Stromberg, K., Hacker, N. F., Cho-Chung, Y. S., and Salomon, D. S. Anti-sense suppression of epidermal growth factor receptor expression alters cellular proliferation, cell-adhesion and tumorigenicity in ovarian cancer cells. Int. J. Cancer, *88:* 566–574, 2000.
5. Pegues, J. C., and Stromberg, K. Inducible antisense inhibition of erbB-2 expression reduces anchorage independent growth of ovarian carcinoma cells. Cancer Lett., *117:* 73–79, 1997.
6. Kallioniemi, A., Kallioniemi, O. P., Sudar, D., Rutovitz, D., Gray, J. W., Waldman, F., and Pinkel, D. Comparative genomic hybridization for molecular cytogenetic analysis of solid tumors. Science (Wash. DC), *258:* 818–821, 1992.
7. Tsao, S. W., Wong, N., Wang, X., Liu, Y., Wan, T. S., Fung, L. F., Lancaster, W. D., Gregoire, L., and Wong, Y. C. Nonrandom chromosomal imbalances in human ovarian surface epithelial cells immortalized by HPV16–E6E7 viral oncogenes. Cancer Genet. Cytogenet., *130:* 141–149, 2001.
8. Abeysinghe, H. R., Cedrone, E., Tyan, T., Xu, J., and Wang, N. Amplification of C-MYC as the origin of the homogeneous staining region in ovarian carcinoma detected by micro-FISH. Cancer Genet. Cytogenet., *114:* 136–143, 1999.
9. Bayani, J., Brenton, J. D., Macgregor, P. F., Beheshti, B., Albert, M., Nallainathan, D., Karaskova, J., Rosen, B., Murphy, J., Laframboise, S., Zanke, B., and Squire, J. A. Parallel analysis of sporadic primary ovarian carcinomas by spectral karyotyping, comparative genomic hybridization, and expression microarrays. Cancer Res., *62:* 3466–3476, 2002.
10. Anand, N., Murthy, S., Amann, G., Wernick, M., Porter, L. A., Cukier, I. H., Collins, C., Gray, J. W., Diebold, J., Demetrick, D. J., and Lee, J. M. Protein elongation factor EEF1A2 is a putative oncogene in ovarian cancer. Nat. Genet., *31:* 301–305, 2002.
11. Loukinov, D. I., Pugacheva, E., Vatolin, S., Pack, S. D., Moon, H., Chernukhin, I., Mannan, P., Larsson, E., Kanduri, C., Vostrov, A. A., Cui, H., Niemitz, E. L., Rasko, J. E., Docquier, F. M., Kistler, M., Breen, J. J., Zhuang, Z., Quitschke, W. W., Renkawitz, R., Klenova, E. M., Feinberg, A. P., Ohlsson, R., Morse, H. C., and Lobanenkov, V. V. Free in PMC BORIS, a novel male germ-line-specific protein associated with epigenetic reprogramming events, shares the same 11-zinc-finger domain with CTCF, the insulator protein involved in reading imprinting marks in the soma. Proc. Natl. Acad. Sci. USA, *99:* 6806–6811, 2002.
12. Lassus, H., Salovaara, R., Aaltonen, L. A., and Butzow, R. Allelic analysis of serous ovarian carcinoma reveals two putative tumor suppressor loci at 18q22–q23 distal to SMAD4, SMAD2, and DCC. Am. J. Pathol., *159:* 35–42, 2001.
13. Hayakawa, A., Wu, J., Kawamoto, Y., Zhou, Y. W., Tanuma, S., Nakashima, I., and Suzuki, H. Activation of caspase-8 is critical for sensitivity to cytotoxic anti-Fas antibody-induced apoptosis in human ovarian cancer cells. Apoptosis, *7:* 107–113, 2002.
14. Menzin, A. W., Loret de Mola, J. R., Bilker, W. B., Wheeler, J. E., Rubin, S. C., and Feinberg, R. F. Identification of oncofetal fibronectin in patients with advanced epithelial ovarian cancer: detection in ascitic fluid and localization to primary sites and metastatic implants. Cancer, *82:* 152–158, 2002.
15. Berns, E. M., Klijn, J. G., Henzen-Logmans, S. C., Rodenburg, C. J., vanderBurg, M. E., and Foekens, J. A. Receptors for hormones and growth factors and (onco)-gene amplification in human ovarian cancer. Int. J. Cancer, *52:* 218–224, 1992.
16. Sartorius, C. A., Takimoto, G. S., Richer, J. K., Tung, L., and Horwitz, K. B. Association of the Ku autoantigen/DNA-dependent protein kinase holoenzyme and poly(ADP-ribose) polymerase with the DNA binding domain of progesterone receptors. J. Mol. Endocrinol., *24:* 165–182, 2000.
17. Munstedt, K., Steen, J., Knauf, A. G., Buch, T., von Georgi, R., and Franke, F. E. Steroid hormone receptors and long term survival in invasive ovarian cancer. Cancer (Phila.), *89:* 1783–1791, 2000.
18. Smith, S., and de Lange, T. Cell cycle dependent localization of the telomeric PARP, tankyrase, to nuclear pore complexes and centrosomes. J. Cell. Sci., *112:* 3649–3656, 1999.
19. Pirrotta, V. Transcription. Puffing with PARP. Science, *299:* 528–529, 2003.
20. Munkarah, A. R., Morris, R., Baumann, P., Deppe, G., Malone, J., Diamond, M. P., and Saed, G. M. Effects of prostaglandin E(2) on proliferation and apoptosis of epithelial ovarian cancer cells. J. Soc. Gynecol. Investig., *9:* 168–173, 2002.